Photo-induced absorption in the pump probe spectroscopy of single-walled carbon nanotubes*

Zhu Zi-Peng(朱子鹏)†

College of Physics and Optoelectronics, Taiyuan University of Technology, Taiyuan 030024, *China*

(Received 22 January 2013; revised manuscript received 25 February 2013)

Femtosecond pump probe spectroscopy is employed to study the photo-induced absorption feature in the single-walled carbon nanotube transient spectrum. The two advantages of the experiment, a chirality enriched sample and tuning the pump wavelength to the resonance of a specific nanotube species, greatly facilitate the identification of the photo-induced absorption signal of one tube species. It is found that a photo-induced absorption feature is located at one radial breathing mode to the blue side of the E_{11} state. This finding prompts a new explanation for the origin of the photo-induced absorption: the transition from the ground state to a phonon coupled state near the E_{ii} state. The explanation suggests a superposition mechanism of the photo-bleach and photo-induced absorption signals, which may serve as a key to the interpretation of the complex pump probe transient spectrum of carbon nanotubes. The finding sheds some light on the understanding of the complex non-radiative relaxation process and the electronic structure of single-walled carbon nanotubes.

Keywords: photo-induced absorption, ultrafast spectroscopy, carbon nanotubes

PACS: 78.67.Ch, 42.65.–k, 78.47.–p **DOI:** 10.1088/1674-1056/22/7/077803

1. Introduction

The boom of the present overwhelming carbon nanotube research dates back to 1991, the year in which Professor Iijima at the NEC corporation reported the historical observation of multi-walled carbon nanotubes.[1] Since the carbon nanotube, especially the single-walled carbon nanotube (SWNT), has been predicted to have many extraordinary properties, such as extremely small size, high tensile strength, high heat transmission capacity, and high current carrying capacity, it has a great potential in the engineering field.[2] On the other hand, it is also a fascinating one-dimensional object that is suited for studying the fundamental aspects of optical, electrical and thermal properties of low-dimensional systems.[3–5]

The optical properties of SWNTs have been intensively studied by using the ultrafast pump probe spectroscopy technique in recent years.[6–15] One intriguing feature in the SWNT transient spectrum is the photo-induced absorption (PA). In the SWNT transient spectrum, the overlap of photo-bleach (PB) and PA signal components of spectrally congested samples makes the interpretation of the spectral features difficult. From the previous reports, the PB features are relatively steady because they correspond to the E_{ii} states of semiconducting SWNTs, which are revealed from the linear absorption spectrum; however, the spectral position and strength of the PA signal vary from report to report. Therefore the understanding of the PA features becomes a key to the understanding of the SWNT transient spectrum. The proposed mechanisms for the origin of the PA features in some previous reports are controversial,[6–12] partly due to the congested spectra of the poly-dispersed SWNT samples used in some investigations, which make it difficult to evaluate the true features from one tube species; partly due to the difficulties of obtaining the narrow band pump and probe beams that are tuned exactly to the E_{ii} states of a specific nanotube species to minimize the interference from all other nanotube species. To date, the origin of the PA signal and its impact on the excited state relaxation process still remain unsatisfactorily understood.

Compared to most of the previous experiments, the experiment presented in this paper has two advantages. One is the use of a chirality enriched SWNT sample. The investigation of spectral transients in the chirality enriched sample overcomes many signal interference problems with poly-dispersed samples and makes a detailed analysis of the spectral features from one tube species possible. The other is the tunability of the excitation wavelength to the resonance of the excited state of a specific tube species, which greatly enhances the signals from one tube species so that the interference from other tube species' signals is reduced. These two advantages make it possible to observe the most detailed signal variations so far of one tube species in the transient spectrum, based on which we propose a new interpretation for the origin of the PA feature, i.e., the transition from the ground state to a phonon coupled state near the E_{ii} states in SWNTs.

*Project supported by the U.S. National Science Foundation (Grant No. DMR0606505).

†Corresponding author. E-mail: zipeng_zhu@yahoo.com

© 2013 Chinese Physical Society and IOP Publishing Ltd

2. Experimental method

2.1. Pump probe experiment setup

The tunability of the excitation wavelength is realized with a wavelength tunable optical parametric amplifier (OPA). Figure 1 shows the setup of the pump probe experiment. Both the pump and the probe pulses are generated in the OPA (Coherent 9450) and have a 50-fs pulse width and a 250 kHz repetition rate. The pump beam (green in the figure) is taken from the signal of the OPA and is tunable from 470 nm to 730 nm with a pulse fluence of up to 0.3 μJ. A computer controlled delay stage (Physik Instrumente, PI-M521.DD) is used to adjust the pump beam delay with a bi-directional reproducibility of position of 0.1 μm = 0.66 fs. The time resolved information is collected by scanning the delay stage to vary the separation between the pump and the probe pulses. After passing through the delay stage, the pump beam is focused into a 1 cm × 1 cm × 5 cm spectrophotometer cell by a lens of 100 mm focal length. The probe beam (red in the figure) is taken from a broadband white light continuum roughly from 400 nm to 1600 nm. It goes through some optical delays and then is also focused into the cell by a spherical reflective optics with a 100-mm focal length. Both the pump and the probe beams at the focus are estimated to be roughly 100 μm in diameter. For alignment purposes, the sample cell is put on an XYZ stage, on which a pinhole with a 100-μm diameter can be attached to facilitate the alignment of the spatial overlap of the pump and the probe beams. The broadband probe beam is dispersed in a spectrometer (Jobin Yvon, triax 320) and detected by a thermoelectrically cooled Si/InGaAs sandwich detector. Optical transients $\Delta T/T_0$ (differential transmission) can be recorded in a computer with a sensitivity of up to 2×10^6 by using the phase sensitive detection of a lock-in amplifier by chopping the pump beam at 1 kHz.

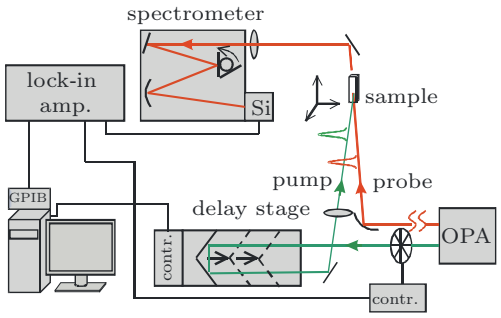


Fig. 1. (color online) Setup of the pump probe experiment.

2.2. Sample preparation

The sample is prepared with a Cobalt–Molybdenum catalyst (CoMoCat) synthesized material[16] that is enriched in the (6, 5) SWNT. The sample purification procedure follows the method described in Ref. [17]. First, 1 mg SWNT soot is mixed with 2 wt.% sodium cholate surfactant in 20 ml water. Then the mixture is ultrasonically agitated in an ice bath using a Branson 450 Sonifier with a tapered microtip at 30% duty cycle for about 2 h. Then a dark suspension is obtained in which micelles formed from sodium cholate molecules wrap and separate individual SWNTs. Next 2 ml of the suspension is put inside the density gradients prepared with iodixanol in a 10 ml centrifugation vial and is then centrifuged in a Sorvall ultracentrifuge with a swinging bucket rotor at 100000g for 12 h. All the dark impurities are then pushed to the bottom of the vial and the (6, 5) tubes form a thin purple band layer in the vial. Lastly, a syringe pump is used to take out 10 to 20 fractions across the purple band with 100–150 μl each and their absorption spectra are analyzed to find the best fraction.

3. Results and discussion

The biggest obstacle encountered when studying the transient spectrum of SWNTs with pump probe spectroscopy and polydispersed samples is the uncertainty of the interference among features from different tube species. In some sense, the detail of the observation is limited by the purity of the sample. Figure 2(a) shows the absorption spectrum of the (6, 5) SWNT enriched sample, in which features from the (6, 5) tube (E_{11} at 990 nm, E_{22} at 570 nm) apparently dominate. Figure 2(b) shows a transient spectrum of the sample in the E_{11} region at 1 ps delay time with the pump wavelength tuned to the E_{22} level illustrated in Fig. 2(a). As a comparison, the corresponding section of the absorption spectrum in Fig. 2(a) is also displayed in Fig. 2(b). The PB feature corresponds to the E_{11} absorption peak position. There is a blue shifted PA signal, whereas there is no red-shifted PA. Questions may be raised: is the position of this PA accidental? And why is there no PA on the red side of E_{11}?

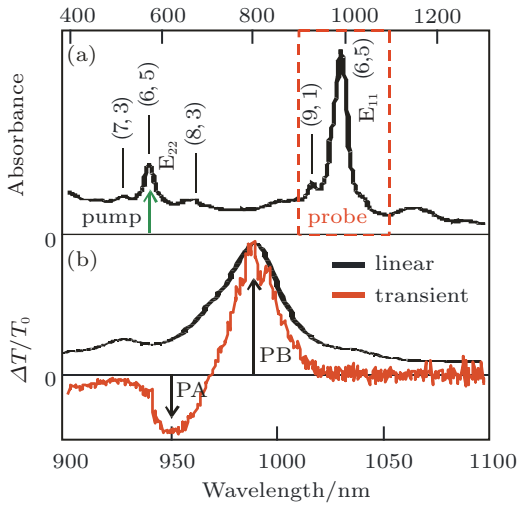


Fig. 2. (color online) (a) Absorption spectrum of the (6, 5) SWNT sample. (b) Comparison of the linear absorption spectrum and the transient spectrum of the sample.

Previous investigations on the PA with the pump probe experiment have provided controversial interpretations.[6–12] Lauret *et al.*[6] observed the PA at nonresonant probe wavelengths and attributed it to a global redshift of the π-plasmon resonance. Korovyanko *et al.*[7] attributed the PA to transitions between bright exciton subbands. Styers-Barnett *et al.*[8] observed a time dependent blue shift of the PB and PA with a SWNT film sample. Ostojic *et al.*[10] attributed the PA to the carrier-induced absorption peak broadening after excitation. And Pedersen *et al.*[9] predicted in a theoretical calculation that there would be a red-shifted PA due to a bi-exciton complex. Lately, Gao *et al.*[12] assigned the PA features to transitions from the lowest level in the E_{11} exciton manifold to levels in the $E_{11}+E_{22}$ biexciton manifold. These many different interpretations of the origin of the PA features suggest that, on one hand, it is a very interesting phenomenon that relates to the fundamental aspects of optical, electrical, and thermal properties of SWNT; on the other hand, it is still far from being satisfactorily understood.

Figure 3(a) shows the pump power dependence of the transient spectrum taken at 1 ps pump probe delay time with the pump wavelength set at the E_{22} resonance of the (6, 5) tube. The main PB peak is near 990 nm and the PA valley is around 950 nm. The PB amplitude of the (6, 5) tube saturates at about 5 mW, while the PB of the E_{11} of the (9, 1) tube near 920 nm continues to grow with increasing power and becomes very pronounced at 13.9 mW.

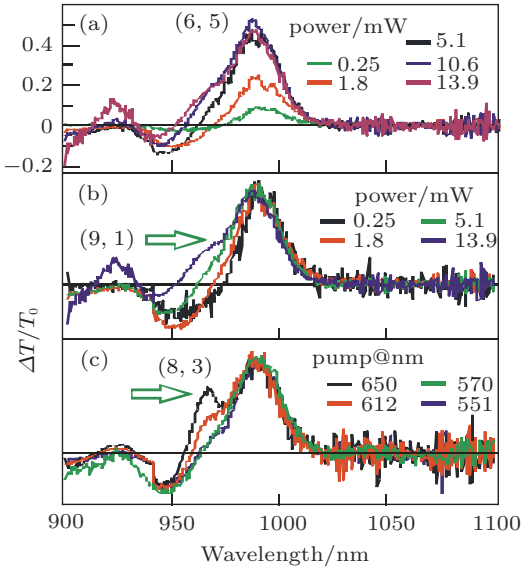


Fig. 3. (color online) Pump power and pump wavelength dependences of the transient spectrum in the E_{11} region of the (6, 5) tube. (a) Pump power dependence of the transient spectrum of the sample. (b) Normalized spectra of those in panel (a). (c) Pump wavelength dependence of the transient spectrum, spectra are normalized.

Figure 3(b) shows some normalized spectra of those in shown Fig. 3(a). The position of the PB peak at 990 nm seems not to move with power. The stability of the PB position under high excitation energies has also been reported with polydispersed SWNT samples.[10] On the other hand, the position of the PA peak moves to the higher energy side and the PA/PB peak value ratio decreases with increasing power. We attribute these changes mainly to the interference caused by the PB signal of the (9, 1) tube at 920 nm. Also there is an abrupt slope change near 960 nm in the transient spectrum at 13.9 mW pump power (pointed by an arrow in Fig. 3(b)), which causes the apparent full width at half maximum (FWHM) of the PB peak at 990 nm to increase.

To investigate the rapid slope change near 960 nm, a pump wavelength dependence study of the transient spectrum is carried out on the same sample, and the normalized spectra are shown in Fig. 3(c). When the pump wavelength is tuned to 650 nm (near the E_{22} of the (8, 3) tube), a clear PB peak appears at 960 nm, which corresponds to the E_{11} of the (8, 3) tube. This result clearly suggests that the variation of the FWHM of the (6, 5) PB peak is affected by the PB of different tube species in the sample, and a PB peak in the transient spectrum has a superposition effect of the PBs from several tubes, which may saturate successively with the pump power. We also notice that the PA position and the PA/PB peak ratio do not vary with the pump wavelength as much as with the pump power.

In all these measurements, the amplitude of the PB is always larger than that of the PA for the (6, 5) tube irrespective of the pump power and the pump wavelength. The variation of the PA position and strength shown in Fig. 3 clearly shows that the features of minority tube species always interfere with those of the majority species even with a purified chirality enriched sample. It suggests that in order to minimize the interferences from minority tube species, it is necessary to pump on the resonance of the E_{ii} states of the majority tube with an appropriate low power. Based on these considerations, the spectrum under 1.8 mW pump power in Fig. 3(b) is selected for further data analysis in Fig. 4.

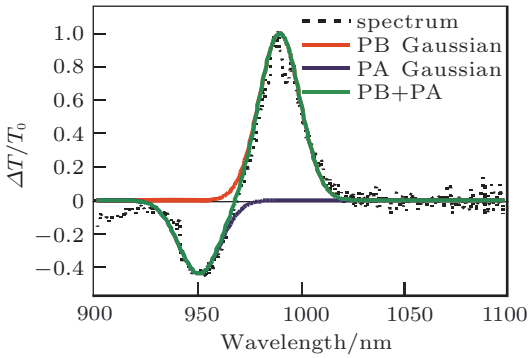


Fig. 4. (color online) The transient spectrum is fitted with the superposition of a PB Gaussian and a PA Gaussian.

In the spectrum shown in Fig. 4, the position of the PA feature "accidentally" falls at the radial breathing mode

(RBM) of the (6, 5) tube.[18] This finding inspires us to raise a hypothesis: the PA feature is actually due to the RBM. To investigate this idea, we then perform a transient spectrum curve fit in Fig. 4.

We use two Gaussian functions to represent the contributions from the PB and the PA signals. The PB Gaussian is centered at the E_{11} state (990 nm), and the PA Gaussian is centered at the RBM position (951 nm). The FWHMs of the PB and PA Gaussians are chosen to be the same (in wavelength), assuming that the state at the RBM is strongly coupled to the E_{11}. The FWHM should be roughly the same in energy for the illustration purposes, but in this wavelength range it will not make a noticeable difference. The amplitudes of the PB and PA are adjusted so that the sum of PA and PB fits the spectrum well.

The unexpected good fitting result in Fig. 4 further inspires us to propose a new interpretation for the origin of the PA signal by means of the density of states (DOS) of carbon nanotubes[19] illustrated in Fig. 5. The PB signal is due to the band edge transition that corresponds to the E_{11} excited state. After the nanotube is excited by the pump pulse, the DOS corresponding to the RBM increases due to the increase of RBM phonons, illustrated with the dash-lined peaks in Fig. 5. The PA signal is due to the transition between these two states and corresponds to the energy of E_{11}+RBM. The states at the band edge and at the RBM level are coupled with RBM phonons. The increase of the RBM population increases the strength of this coupling, and the coupling between a low DOS state and a high DOS state increases the DOS of the former state. Since the DOS at the RBM level is increased, consequently the probability of the optical transition between the two states increases, resulting in an increased absorption compared with the unexcited condition.

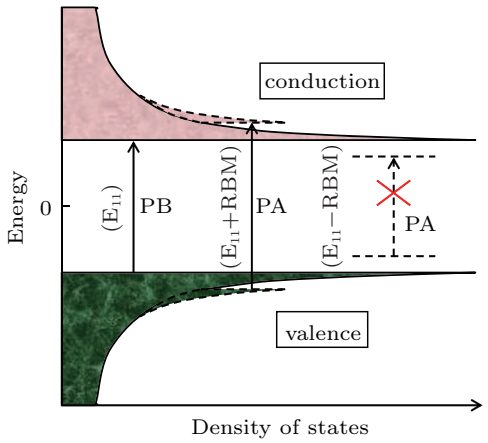


Fig. 5. (color online) Illustration of the origin of the PA signal in E_{11} region.

There is still one unanswered question: why is there is a PA at the blue side of the E_{11} but no red-shifted PA feature? Our hypothesis is that the optical transition is not allowed below the E_{11} energy because it is in the forbidden band (illustrated with a red cross in Fig. 5). In other words, the hot RBM phonon makes the allowed transition more expedite, but it does not lift the barrier of an unallowed transition. This hypothesis does not agree with the excitonic band structure in which there is no one photon allowed state between the E_{11} and the continuum band, and the energy difference between the two (called exciton binding energy) is much bigger than the RBM for the (6, 5) tube.[20] Rather it agrees better with the band structure derived from the tight binding approximation.[19] This hypothesis, of course, awaits further experimental and theoretical investigations for verification.

The main idea of the above mentioned PA origin hypothesis is the RBM phonon assisted coupling between the E_{11} and E_{11}+RBM excited states. The strong coupling between these two states is supported by the similar dynamics at these two states. In Fig. 6, the cross correlation signal of the PB at 988 nm is plotted, that of the PA at 948 nm (reverted and normalized for comparison purpose) is also plotted. The almost overlapped signals suggest that the two states are strongly coupled, and the charged particles at those two states may basically share a common decay channel.

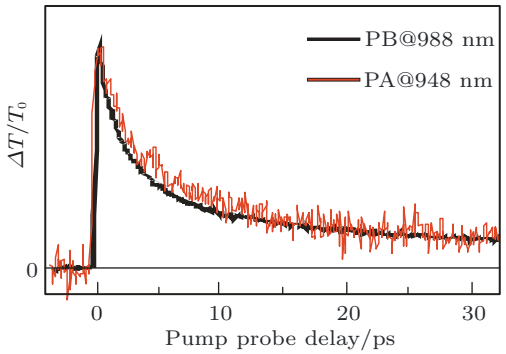


Fig. 6. (color online) Comparison of cross correlations of PB and PA (reverted and normalized) near the E_{11} region.

4. Summary

The most interesting finding in this report is that a PA feature is located at an RBM energy from the E_{11} state. The finding is achieved with two advantages of our experiment, the chirality enriched SWNT sample and the tunability of the excitation wavelength, which facilitate the identification and measurement of PA features of one tube species. The finding leads naturally to the hypothesis that the PA feature is due to the transition between phonon coupled states in the DOS picture. The good spectrum curve fitting in Fig. 4 and the comparison of PA and PB dynamics in Fig. 6 further support the hypothesis. The findings and the proposed hypothesis open a new window for the investigation of the complex non-radiative decay process and the electronic structure of the quasi-one-dimensional SWNT material.

References

[1] Iijima S 1991 *Nature* **354** 56
[2] Collins P G and Avouris P 2000 *Scientific American* **283** 62
[3] Long Y B, Song L, Zhang C Y, Wang L, Fu P M, Zhang Z G, Xie S S and Wang G P 2005 *Chin. Phys.* **14** 2137
[4] Yang J, Dong Q L, Jiang Z T and Zhang J 2010 *Chin. Phys. B* **19** 127104
[5] Miao L, Liu H J, Hu Y, Zhou X, Hu C Z and Shi J 2010 *Chin. Phys. B* **19** 016301
[6] Lauret J S, Voisin C, Gassabois G, Delalande C, Roussignol P, Jost O and Capeset L 2003 *Phys. Rev. Lett.* **90** 057404
[7] Korovyanko O J, Sheng C X, Vardeny Z V, Dalton A B and Baughman R H 2004 *Phys. Rev. Lett.* **92** 017403
[8] Styers-Barnett D J, Ellison S P, Park C, Wise K E and Papanikolas J M 2005 *J. Phys. Chem. A* **109** 289
[9] Pedersen T G, Pedersen K, Cornean H D and Duclos P 2005 *Nano Lett.* **5** 291
[10] Ostojic G N, Zaric S, Kono J, Moore V C, Hauge R H and Smalley R E 2005 *Phys. Rev. Lett.* **94** 097401
[11] Zhu Z, Crochet J, Arnold M S, Hersam M C, Ulbricht H, Resasco D and Hertel T 2007 *J. Phys. Chem. C* **111** 3831
[12] Gao B, Hartland G V and Huang L 2012 *ACS Nano* **6** 5083
[13] Huang L, Pedrosa H N and Krauss T D 2004 *Phys. Rew. Lett.* **93** 017403
[14] Huang L and Krauss T D 2006 *Phys. Rev. Lett.* **96** 057407
[15] Russo R M, Mele E J Kane C L, Rubtsov I V, Therien M J and Luzzi D E 2006 *Phys. Rev. B* **74** 041405(R)
[16] Resasco D E, Alvarez W E, Pompeo F, Balzano L, Herrera J E, Kitiyanan B and Borgna A 2002 *J. Nanoparticle Res.* **4** 131
[17] Arnold M S, Stupp S I and Hersam M C 2005 *Nano Lett.* **5** 713
[18] Bachilo S M, Strano M S, Kittrell C, Hauge R H, Smalley R E and Weisman R B 2002 *Science* **298** 2361
[19] Saito R, Dresselhaus G and Dresselhaus M S 1998 *Physical Properties of Carbon Nanotubes* (London: Imperial College Press)
[20] Wang F, Dukovic G, Brus L E and Heinz T F 2005 *Science* **308** 838